Studies on Semibatch Microemulsion Polymerization of Butyl Acrylate: Influence of the Potassium Peroxodisulfate Concentration

Alberto G. Ramírez,[†] Raúl G. López,*[,†] and Klaus Tauer[‡]

Centro de Investigación en Química Aplicada, Blvd. Enrique Reyna 140 CP 25100, Saltillo, México, and Max Planck Institute of Colloids and Interfaces, Am Mühlenberg D-14476 Golm, Germany

Received April 14, 2003; Revised Manuscript Received October 16, 2003

ABSTRACT: Semibatch microemulsion polymerization of butyl acrylate in the presence of sodium dodecyl sulfate/Aerosol OT surfactant mixture and potassium peroxodisulfate as initiator is analyzed with respect to particle nucleation and growth. It is concluded that particle nucleation occurs during the whole batch and semibatch polymerization periods also in the absence of micelles. The observed increase in the polymer content compared to the batch microemulsion polymerization is mainly due to nucleation of new particles during the semibatch stage. During the post-addition polymerization period particle growth is dominated by particle coalescence. The particular method of semibatch microemulsion polymerization allows to obtain latexes with particle sizes below 40 nm (dynamic light scattering intensity weighted diameter) at polymer concentrations near to 30 wt % and stabilizer amounts between 5 and 6% relative to the polymer mass.

Introduction

Over the past decades a clear tendency is to recognize toward the development of polymer latexes with steadily decreasing average particle sizes. This is mainly due to following reasons. Latexes with average particle sizes below 100 nm allow to take best advantage of the compartmentalization effects in heterophase polymerization where a particle contains either one or none radical (the average number of radicals per particle is 0.5 or smaller), and both a high rate of polymerization and a high molecular weight can be realized at the same time. Furthermore, small size latex particles allow the formation of mixed and hybrid systems on length scales, which are only hardly accessible by simple mechanical mixing such as grinding or stirring. For instance, the smaller the particle size, the better is the incorporation of costly pigments during film formation. Moreover, smaller particles penetrate better and easier to substrates than larger ones. However, the price to pay for particles with smaller sizes is the higher stabilization efforts, which are necessary at given solids content. High solids, small size latexes need also special precautions with regard to colloidal stability and control of rheology due to enhanced particle−particle interactions. Note the average interfacial distance between two particles scales with the inverse cubic root of the particle number.

Polymerization of Winsor IV microemulsion prepared of hydrophobic monomers is an easy way to get latex particles with average sizes well below 50 nm in diameter. The main drawbacks of this type of microemulsion polymerization are an extraordinarily high surfactant-to-monomer ratio (larger than 1) and a low monomer concentration with respect to water (low solids content of the final latexes). Both facts counteract the commercial utilization of microemulsion polymerization. Consequently, efforts have been undertaken to increase the solids content and to reduce the surfactant content in microemulsion latexes, which can be subdivided into three different routes. The first way is the search for more effective surfactant systems in the sense that the concentration range of the microemulsion phase is shifted toward lower surfactant and higher monomer parts in the overall mixture such as in refs 1 and 2. These papers refer to special Y-shaped surfactants that is sodium salts of 12-butinoyloxy-9-octadecenate[1] or 12-hexinoyloxy-9-octadecenate,[2] which allow the formulation of Winsor IV microemulsions with butyl acrylate and styrene, respectively, with increased monomer concentrations compared to nonbranched surfactants such as alkyltrimethylammonium halide emulsifiers. The second possibility is to start with a Winsor IV microemulsion and to overlay the microemulsion phase with an additional layer of neat monomer (which is finally a system very similar to a Winsor I microemulsion).[3] The authors describe the procedure exemplarily for polymerization of styrene microemulsion formed with dodecyltrimethlyammonium bromide as surfactant. The polymerization was carried out at 30 °C with the ammonium peroxodisulfate/*N*,*N*,*N*′,*N*′-tetramethylethylenediamine redox initiating system. The stirrer speed was low enough to keep the bulky monomer phase and to restrict the polymerization to the underlying microemulsion phase. The authors could realize polystyrene content of about 15% and the number-average particle size determined by enumerating transmission electron micrographs was about 80 nm. The third route is the one with the highest probability of a potential technical realization because it comprises various kinds of semibatch procedures as they are frequently applied in industrial emulsion polymerizations (cf. ref 4). To the best of the authors' knowledge, the oldest description of semibatch microemulsion polymerization can be found in a patent applied in 1989.[5] Examples in this patent describe incremental addition (either batchwise addition or continuous feed) of microemulsions for instance with Dowfax 2A-1 as emulsifier and acrylamide as costabilizer to either aqueous initiator solution or microemulsion. Exemplarily, a butyl acrylate microemulsion was obtained with 41% solids content and intensity-weighted average particle size of about 52 nm

[†] Centro de Investigación en Química Aplicada.
[‡] Max Planck Institute of Colloids and Interfaces.
* Corresponding author: Fax (844) 4-38-98-39; e-mail glopez@polimex.ciqa.mx.

10.1021/ma030218g CCC: $27.50
Published on Web 03/20/2004

at about 5.5% stabilizer (Dowfax2A-1 plus acrylamide) with respect to the mass of butyl acrylate. In the following years several papers have been published dealing with semibatch microemulsion polymerizations.[6−12] The main variables in these investigations are the kind of feeding the monomer with respect to the composition of the feed stream and the addition mode. The monomer can be fed either as neat substance or as emulsion with the same or different composition compared with the starting microemulsion. The addition mode can be either stepwise in batches or continuously. For instance, the influence of the kind of monomer was investigated for microemulsions formed with sodium dodecyl sulfate (SDS) as emulsifier and 1-pentanol as costabilizer.[8] The polymerization was started with the ammonium peroxodisulfate/*N*,*N*,*N*′,*N*′-tetramethylethylenediamine redox system at 40 °C whereby after a prebatch period neat monomer was added continuously over a duration of 2−3 h. For styrene, butyl methacrylate, butyl acrylate, methyl methacrylate, and methyl acrylate the maximum total monomer mass in g, the number-average particle size in nm, and the monomer-to-SDS ratio were 10 g, 10 g, 15 g, 16 g, 30 g; 46.8 nm, 19.8 nm, 16.5 nm, 15.3 nm, 14.5 nm; and 6.7, 7.1, 10.7, 11.4, 30, respectively. These data clearly confirm the influence of the monomer polarity in the sense that obviously the more polar monomers can act as cosurfactant, thus shifting the microemulsion range toward higher monomer and lower surfactant concentration and moreover leading to smaller particles. Examples for a stepwise monomer addition can be found in ref 7 where styrene is polymerized in aqueous microemulsions with dodecyltrimethylammonium bromide as surfactant and 2,2′-azobis(2-amidinopropane) dihydrochloride (V50) as initiator. The starting microemulsion composed of 6 wt % styrene, 14.1 wt % surfactant, and 79.9 wt % water is polymerized at 60 °C batchwise for about 1 h before five batches of 5 mL of styrene were added every 20 min. The final conversion and solids content was about 90% and 40%, respectively, and the hydrodynamic particle size increased during the semibatch period from 26.2 to 45.1 nm. Another example of batchwise monomer addition has been published for vinyl acetate microemulsions.[11] The starting microemulsion was formed with Aerosol OT as surfactant (weight ratio to water 1/99) and 3 wt % of monomer. During the semibatch period six batches of vinyl acetate were added hourly. The final solids content and the hydrodynamic particle diameter were about 30% and 70 nm, respectively. As the polydispersity of the particle size distribution remained almost unchanged, the authors concluded that no secondary nucleation took place during the second polymerization stage. But at higher solids content chain transfer to polymer occurred as the polydispersity of the molecular weight distribution was increasing. Finally, an example is given describing the preparation of stimuli-responsive polyelectrolytes and polyampholytes in water in oil microemulsions with Isopar M as continuous phase.[12] The surfactant concentration could be minimized and the polymer content maximized by choosing a proper surfactant system on the basis of the cohesive energy ratio concept. The monomer was fed in form of a microemulsion having the same composition as during the initial batch stage. The amount of surfactant could be reduced from 14 to 8 wt % at 20% solids content.

Table 1. Polymerization Recipes and Procedures

component	batch (g)	semibatch (g)	feeding time (min)
ME1	B1	SB1	
water	97.216		
SDS	1.488		
AOT	0.496		
KPS	0.007		
BA	0.8	38.78	70
ME2	B2	SB2	
water	97.216		
SDS	1.488		
AOT	0.496		
KPS	0.012		
BA	0.8	32.067	45
ME3	B3	SB3	
water	97.216		
SDS	1.488		
AOT	0.496		
KPS	0.017		
BA	0.8	34.78	45

In conclusion, semibatch microemulsion polymerization is a way on one hand to get polymer dispersions with average particle size in the range of 50 nm and on the other hand to increase the solids content and to reduce the surfactant content with respect to polymer mass compared to "classical" batch microemulsion polymerizations. However, the goal to get as small as possible particle sizes sets automatically limits with regard to the maximum solids content and minimum amount of surfactant.

The aim of this contribution is to report results on the preparation of microlatexes of poly(butyl acrylate) with high solids content and low surfactant concentration. The monomer was charged into the reactor in two steps. The first step is a normal batch polymerization of a microemulsion made of a mixture of sodium dodecyl sulfate (SDS) with sodium bis(2 ethylhexyl)sulfosuccinate (Aerosol OT or AOT) in a weight ratio of 3 as surfactant system, water as continuous phase, and the monomer. The polymerizations were initiated with the water-soluble initiator potassium peroxodisulfate (KPS) at different concentrations. The second step is the addition of neat monomer and is started when the conversion of the first polymerization reaches its final value (above 95%). The feeding rate of the butyl acrylate monomer (BA) was chosen directly proportional to the initiator concentration. The development of polymer content, particle size, particle number, and molecular weight were investigated during the semibatch period. Furthermore, emphasis is placed on changes of colloidal properties during the course of the polymerization and related to the polymerization mechanism.

Experimental Part

Materials. AOT (98% from Fluka) was used as received. SDS (99% from Aldrich) and KPS (Wako Chem.) were both recrystallized from methanol. Butyl acrylate (Aldrich) was distilled under reduced pressure and stored at 4 °C in a refrigerator. Prior to use the monomer was checked regarding oligomer formation during storage by instilling a drop into an excess of methanol. Only oligomer-free monomers were used. The water was taken from a Seral purification system (PURELAB Plus) with a conductivity of 0.06 μS cm^{-1} and degassed prior to use for the polymerizations.

Polymerization Process. Polymerizations were carried out at 60 °C in a 200 mL jacketed glass reactor equipped with a reflux condenser and inlets for nitrogen, monomer feed, and mechanical agitation. A 45° pitched down flow four-bladed impeller was used with a stirrer speed of 600 rpm. Polymerization recipes and procedures are summarized in Table 1. The

microemulsion polymerizations carried out comprise three directly consecutive periods: the initial batch period (B1−B3 in Table 1), the semibatch or semicontinuous period while additional monomer is fed into the reactor (SB1−SB3 in Table 1), and the final post-addition polymerization period (PA). A typical procedure includes the preparation of a microemulsion composed of 0.8 g of BA, 1.488 g of SDS, 0.496 g of AOT, and 92.2 g of water. The use of the mixture SDS/AOT in a weight ratio of 3 obeys to that AOT enhances the normal microemulsion region of the systems stabilized with only SDS.[13] The microemulsion was stirred, heated to 60 °C, and argon bubbled through it for 30 min. To start the reactions, the required amount of KPS dissolved in 5 g of water was added to start the polymerization. Once the conversion attained a stable value at the end of the seeded or batch period, feeding of BA monomer was started using a syringe pump. The monomer flux and the length of the addition period were varied in dependence on the initial KPS concentration (cf. Table 1). The monomer flux was stopped when the viscosity in the reactor became so high that an efficient stirring was not possible anymore. At this point the dispersion had the appearance similar to a high viscous gel. During the semibatch period argon was continuously bubbled through the reaction mixture. After the monomer addition was stopped the reaction was allowed to complete for a period of 1.5 h, which was the same for all three recipes investigated. The post-addition period in fact is another batch polymerization period. Samples were taken during the whole polymerization process to follow conversion gravimetrically and for measuring particle sizes and molecular weight. The instantaneous conversion at time t_i during the addition period was calculated from the actual polymer content relative to the amount of monomer fed in the reactor until t_i. For calculations of instantaneous conversion, the weights of the previously taken samples were considered.

Particle Size Determination. Particle size was measured at 25 °C and a scattering angle of 90 °C with a Nicomp 370 (V12.0; Santa Barbara, CA) dynamic light scattering (DLS) apparatus equipped with a 5 mW He−Ne laser ($\lambda = 632.8$ nm). Intensity correlation data were analyzed by the method of cumulants to provide the average decay rate, $\langle\Gamma^2\rangle$ ($= q^2D$), where $q = (4\pi n/\lambda)\sin(\theta/2)$ is the scattering vector, n is the refractive index of the continuous phase, D is the translational diffusion coefficient, and θ is the scattering angle. The measured diffusion coefficients were to calculate the apparent diameters by means of the Stokes−Einstein relation assuming that the continuous phase has the viscosity of water. Latexes were diluted up to 35 times and filtered through 0.25 μm Millipore filters before QLS measurements in order to minimize particle interactions and to remove dust particles. Thus, the average particle diameters (D_p) used throughout are the intensity-weighted average diameters. Particle numbers have been calculated from the polymer content and D_p.

Molecular Weight Determination. Weight-average molecular weights of polymer samples were determined by light scattering with a HNA-50 Carl Zeiss Jena apparatus equipped with a He−Ne laser ($\lambda = 632.8$ nm). Previously, the latexes were dialyzed against distilled water over a period of 1 week. While dialysis the water was refreshed daily. After removing most of the stabilizers, initiator residuals, and water-soluble oligomers by dialysis, the polymer was isolated by precipitating the latex in an excess of methanol. The polymer was dried in a vacuum at 40 °C for 24 h, dissolved in acetone at various concentrations, centrifuged, and filtered through 0.25 μm Millipore filters before the measurements. The molecular weights (M_w) were calculated from Zimm plots according to standard procedures.

Results and Discussion

General Considerations−Overall Polymerization Behavior. Peculiarities of the batch microemulsion polymerization of BA with the mixed emulsifier system SDS/AOT have been discussed in detail elsewhere.[13] A comprehensive investigation by means of reaction calorimetry and dynamic light scattering revealed unexpected results with regard to polymerization kinetics and colloidal properties of the final latexes. Particularly, with increasing surfactant concentrations a decrease in the overall rate of polymerization accompanied by an increasing incubation time of the polymerization and increasing average particle sizes in the final latexes has been observed. All these experimental results could be explained consistently with a particle nucleation mechanism based on the classical nucleation theory.

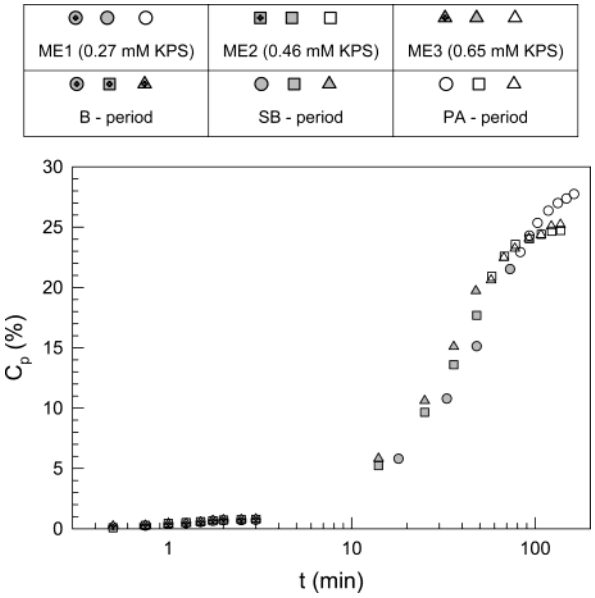

Figure 1. Change of polymer content (C_p) with time during overall microemulsion polymerizations in dependence on initiator concentration. Legend: cf. experimental part and Table 1.

The duration of a batch microemulsion polymerization under the particular conditions is extremely short. For instance, 2 g of BA in the former investigations was polymerized within less than 10 min. In the present experiments with 0.8 g of BA used in the batch periods a conversion above 95% is reached within 2 or 3 min depending on the initiator concentration. During the feeding period the instantaneous conversion decreases to values between 60 and 75%; that is, monomer is accumulated in the reactor as it swells micelles and existing particles but not in form of droplets. Then, during the post-addition period the conversion increases to values between 95 and 99%.

Figures 1−3 illustrate the whole course of the microemulsion polymerizations with regard to the polymer content (C_p) that is the mass of polymer in the whole reaction mass (Figure 1), the average particle diameter (Figure 2), and the average particle number per unit volume continuous phase that is water (Figure 3). On one hand, these data reveal the dramatic changes during semibatch microemulsion polymerizations, and on the other hand they prove that this polymerization variant obviously exhibits a variety of interesting kinetic and colloidal features, which will be subsequently discussed in detail. For instance, during the batch period, which in fact is a classical microemulsion polymerization, the average particle size and the average number of polymer particles decreases and increases, respectively. This is the expected behavior as it was also observed for BA microemulsion polymerizations with the SDS/AOT surfactant combination however at both

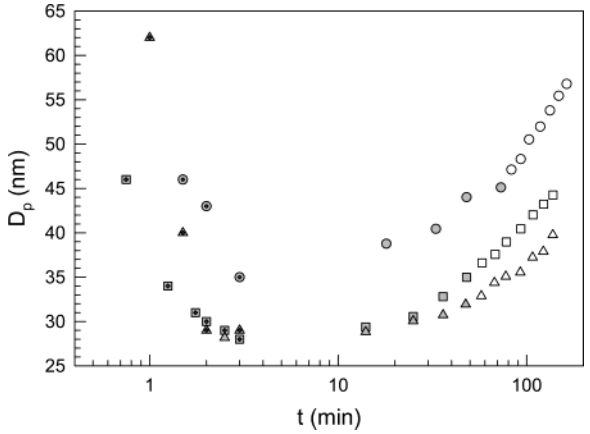

Figure 2. Change of average particle diameter (D_p) with time during overall microemulsion polymerizations in dependence on initiator concentration. Legend: cf. Figure 1.

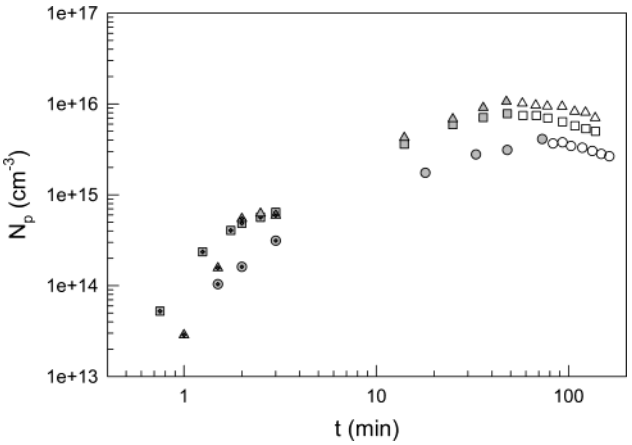

Figure 3. Change of average particle number (N_p) with time during overall microemulsion polymerizations in dependence on initiator concentration. Legend: cf. Figure 1.

higher surfactant and monomer concentration (cf. ref 13). Then, during the subsequent periods both the average particle size and the average particle number increase. Whereas D_p increases throughout the whole remaining course of the polymerization, the particle number starts at the end of the semibatch period to drop. As the drop in the particle number does not lead to macroscopic coagulation, the process is considered as particle coalescence resulting in spherical particles with still colloidal dimensions. Despite gradual differences this general behavior is independent of the initiator concentration. The final latexes are fairly high concentrated polymer dispersions with average particle sizes below 60 nm whereas at the highest initiator concentration the average particle size is even below 40 nm. The surfactant concentration relative to the amount of monomer is between 5 and 6 wt %. This is a considerable improvement regarding the emulsifier utilization compared with classical microemulsion polymerizations, and moreover the values reached are absolutely comparable with that obtained for similar sized latexes prepared in batch emulsion polymerizations. Although the particular polymerization procedure resembles seeded emulsion polymerizations, there is at least one fundamental difference. When the microemulsion batch period ends, the free emulsifier concentration in the reactor is still above the critical micelle concentration (cmc) that is empty micelles are present at the beginning of feeding additional monomer into the reactor (cf. ref 13). The

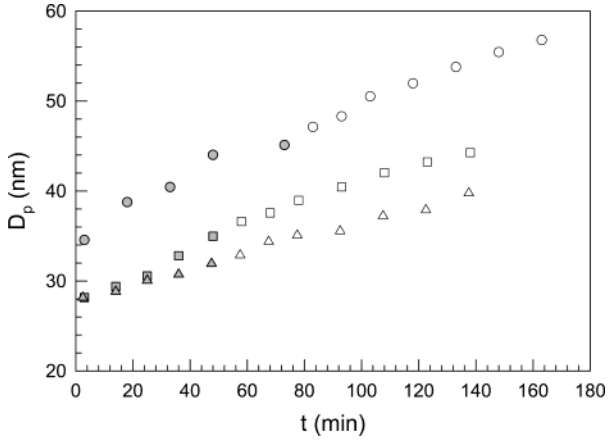

Figure 4. Change of average particle size during monomer feeding and post-addition period. Legend: cf. Figure 1.

empty micelles compete with the polymer particles for the monomer, and hence a situation is reached favoring both the formation of new latex particles and the volume growth of the previously formed, quasi-seed particles. Figures 2 and 3 reveal that both processes really take place as the number of particles increases from some 10^{14} cm^{-3} at the end of the batch period to almost 10^{16} cm^{-3} at the end of the feeding, and the average particle size increases from 34.6 to 45.1 nm and 28.2 to 32 nm for the lowest and highest KPS concentration, respectively. This change of N_p and D_p in the same direction is a fundamental difference compared with microemulsion batch polymerization period where both parameters are changing oppositely directed.

The data with regard to the development of polymer content, average particle size, and average particle number already show that unlike during seeded emulsion polymerization in seeded microemulsion polymerization most of the increase in the polymer content is realized by newly formed particles and not by growth of seed particles.

Development of the Average Particle Size. The change of the average particle size of unswollen and spherical polymer particles during any kind of heterophase polymerization should occur according to relations 1−3.

$$V_p = \frac{\pi}{6} D_p{}^3 N_p \tag{1}$$

$$X = \frac{V_p}{M_{m0}/\rho_p} \times 100 \tag{2}$$

$$\frac{dD_p}{dt} \propto \frac{1}{N_p D_p{}^2} \frac{dV_p}{dt} - D_p \frac{dN_p}{dt} \tag{3}$$

V_p is the overall polymer volume, X is the overall conversion, M_{m0} is the total mass of monomer, r_p is the polymer density, and t is the time. According to these relations, the shape of the particle size−time curve depends on the overall rate of polymerization and the change of the particle number with polymerization time, and hence, it is not easily to predict. Figure 4 shows enlarged D_p−t curves for the semibatch and the final polymerization periods. The remarkable result is that these curve follow within the experimental scatter almost straight lines even until the end of the polymerizations where the rate of polymerization converges to

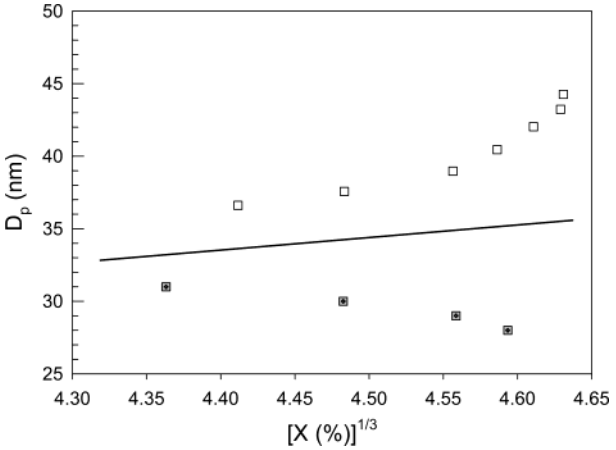

Figure 5. Change of the average particle size with the cubic root of the conversion for ME2 during the batch period (gray squares with x-hair) and during the post-addition polymerization stage (white squares); the straight line indicates particle growth under the condition of constant particle number.

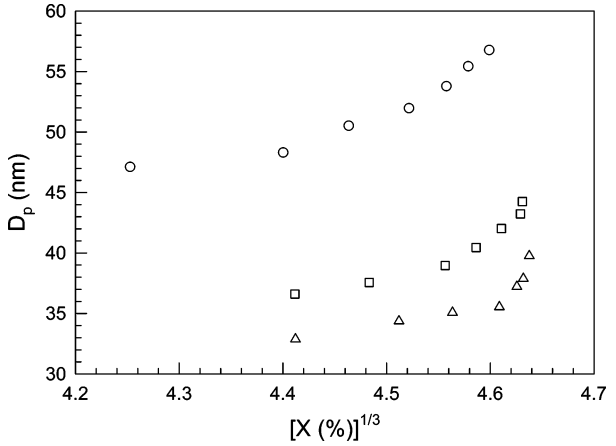

Figure 6. Change of average particle diameter with the cube root of the conversion during the post-addition polymerization period. Legend: circles, ME1 (0.27 mM KPS); squares, ME2 (0.46 mM KPS); triangles, ME3 (0.67 mM KPS).

zero, and hence, also particle growth by monomer consumption is expected to vanish. Clearly, this behavior is the result of the peculiarity of the semibatch microemulsion polymerization process where particle growth by monomer consumption and changes in the particle concentration—either particle nucleation or particle coalescence—occur simultaneously during the whole duration of the reaction.

In the case of an ideal seeded polymerization that is with constant number of seed particles the D_p-t curve should reflect the changes in the rate of polymerization. Moreover, the plot D_p vs $X^{1/3}$ should give a straight line as a consequence of $dN_p/dt = 0$. If, however, dN_p/dt is not constant its sign determines the direction of the deviation from the straight line. Figure 5 shows exemplarily such plots of the batch period and the final polymerization stage for ME2. Both sets of data points clearly deviate from the straight line, thus indicating $dN_p/dt > 0$ and $dN_p/dt < 0$ for the initial batch and the final polymerization period, respectively. An enlargement of the $D_p-X^{1/3}$ curves during the post-addition period as depicted in Figure 6 reveals that the positive deviation from a straight line is larger for smaller particles or larger initiator concentration. These curves together with the plots in Figure 3 suggesting that particle coalescence processes are taking place at least

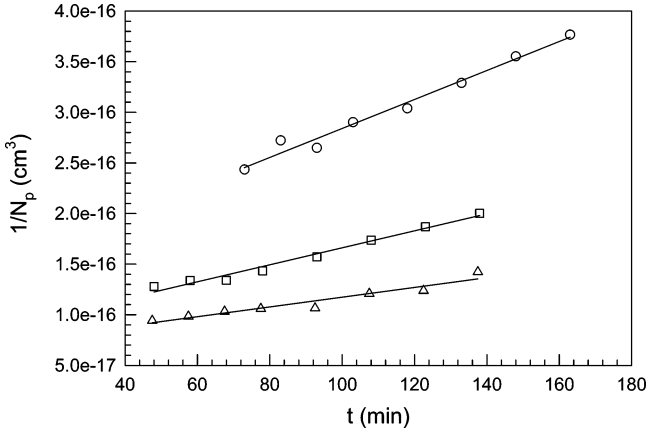

Figure 7. Second-order plots for the determination of the coalescence rate constants according to eq 4: points, experimental data; lines, linear regression. Legends: cf. Figure 1.

after the monomer feed has been stopped. Unfortunately, a detailed analysis of the development of the average particle size according to eq 3 is presently impossible mainly due to the fact that it is experimentally not possible to determine whether particle nucleation and coalescence take place simultaneously or not.

Particle Coalescence during the Post-Addition Period. Before discussing the overall development of the N_p-t curves, the decrease in the particle number during the last polymerization stage will be treated separately as with decreasing monomer concentration particle nucleation becomes more and more unlikely, and the particle coalescence is effectively the sole process determining particle growth (cf. Figure 6). Particle coalescence requires a close contact between the particles, a rupture of the stabilizing surfactant layer, and finally the confluence of the particles. Such processes can be treated quantitatively assuming a second-order reaction as given by eq 4 (cf. ref 14 and references therein), where r_c is the rate of coalescence that is basically the rate of a two-particle contact and k_c is the rate constant.

$$r_c = -\frac{dN_p}{dt} = k_c N_p^{\,2} \tag{4}$$

With experimental particle number−time curves it is possible to calculate k_c from N_p^{-1}−time plots according to standard kinetics. Figure 7 shows these plots for the post-addition periods of the BA microemulsion polymerizations. For all initiator concentrations (C_I) the experimental data points result in straight lines where from the slopes k_c values of 1.43×10^{-18}, 8.39×10^{-19}, and 4.81×10^{-19} cm^3 min^{-1} for KPS concentrations of 0.27, 0.46, and 0.63 mM have been calculated. The k_c values show a clear dependence on the initiator concentration that is they are higher the lower C_I according to $k_c \propto C_I^{-1.22}$. This dependence might be surprising as one would expect a decrease in latex stability with increasing C_I due to the increase in the ionic strength which for electrostatically stabilized colloids decreases the repulsive potential between the particles (cf. ref 15). To explain this experimentally determined dependence, one has to consider that the majority of charges stabilizing the particles arise from adsorbed stabilizer molecules. The adsorption characteristics of emulsifiers strongly depend on the ionic strength. For instance, increasing ionic strength causes surfactant monolayers to condense

more strongly; that is, the surface coverage increases as it was also shown for SDS solutions.[16] In a comprehensive study on the effect of increasing ionic strength on the adsorption behavior of tritiated SDS, it was shown that with increasing amount of sodium chloride both the cmc and the area occupied per SDS molecule decreases and the adsorbed amount per unit area increases.[17] The above experimental data have been used to verify also theoretically that at given surfactant concentration increasing ionic strength in the continuous phase causes on one hand the surface pressure at the air−water interface, the adsorbed amount of both surface active and counterions, and the occupancy of the Stern layer by counterions to increase but on the other hand the surface potential to decrease.[18] Regarding the decrease in the surface potential it is to note that the theory predicts based on the above experimental data for tritiated SDS at a concentration of 10^{-3} M a decrease in the surface potential at the air−water interface from about −170 mV to about −90 mV at an ionic strength of 115 mM sodium chloride. However, under the same conditions the adsorbed amount of either kind of ions increases by almost a factor of 10. In light of these results the measured inverse proportionality between the coalescence rate constant and the KPS concentration can be explained by a denser surfactant adsorption layer at higher ionic strength resisting the rupture of the surfactant film during the particle coalescence process. Results which could be understood in a similar way have been published for batch microemulsion polymerizations of styrene with dodecyltrimethylammonium bromide as surfactant and KPS or V50 as initiator at variable ionic strength.[19] The authors observed decreasing average particle sizes (increasing average particle numbers) with increasing ionic strength. These results can be explained on the basis of the above results of increasing adsorption of surfactant molecules with increasing ionic strength. At increasing ionic strength the surfactant molecules try to avoid more and more contact with water, and hence they will either self-assemble in the form of micelles or adsorb at hydrophobic interfaces. Thus, increasing ionic strength causes a higher concentration of however smaller particles. Using exactly the same arguments, another possibility to explain decreasing particle sizes with increasing ionic strength is to consider particle nucleation within the frame of classical nucleation theory where higher ionic strength may cause increased nucleation due to the salting-out effect (cf. refs 13, 20, and 21).

As the final BA polymer dispersions are stable at ambient conditions for a long period of time, the observed decrease in the particle number is somehow connected with the polymerization reaction at elevated temperatures. Similar reaction-mediated particle coalescence was also observed during batch emulsion polymerizations of vinyl chloride with SDS as emulsifier at concentrations below and above the cmc and also during emulsifier-free polymerizations.[14] In contrast to the results discussed here, the N_p^{-1}−time plots in the case of vinyl chloride emulsion polymerization are not linear, but the slope is decreasing continuously throughout the whole reaction, which means that there is no simple coalescence rate constant as predicted by eq 4 deducible. It turned out that the experimental data could be modeled pretty well assuming that additionally to the close contact between the particles the radical desorption out of one of the contacting particles is the rate-determining step for particle coalescence. With this assumption, which is because of the high radical transfer reaction rate to monomer in vinyl chloride free radical polymerizations and the subsequent high radical desorption rate, causing the low average number of radicals per particle, fairly reasonable, it was possible to derive a modified eq 5 to model particle coalescence successfully in the course of vinyl chloride emulsion polymerization.[14] k_{c1} is a modified rate constant depending on the particular reaction conditions such as initiator and emulsifier concentration but also on the diffusion coefficient of the exiting radical within the particles. This behavior is a typical example for reaction-mediated particle coalescence.

$$r_c = -\frac{dN_p}{dt} = k_{c1} D_p^{-2} N_p^{2} \tag{5}$$

In what way this mechanism is also applicable to explain the data described here for BA semibatch microemulsion polymerization is not clearly to decide. On one hand, it is to note that eq 5 describes a strong dependence of the coalescence rate on the inverse particle size, which was indeed experimentally observed for vinyl chloride emulsion polymerization. However, this seems obviously not the case for BA as a single k_c value is obtained for one particular polymerization, and moreover the polymerization leading to the largest particles exhibits also the largest k_c values. On the other hand, also for BA free-radical polymerization chain transfer to monomer plays a role causing low average number of radicals per particle and hence proving radical desorption. The transfer constant for BA to monomer is 1.56 L mol^{-1} s^{-1} at 50 °C[22] and hence about a factor of 6 lower than that for vinyl chloride.[23]

Consequently, it is on one hand not to exclude that the lower chain transfer rate to monomer of BA compared to vinyl chloride causes the different behavior regarding the size dependence of the coalescence rate, but in both cases radical desorption may lead to a rupture of the stabilizing surfactant film and thus contributing to the observed reaction-mediated particle coalescence. On the other hand, it may also be very likely that in the case of BA heterophase polymerization the close contact between two particles as described by eq 4 is already sufficient to cause particle coalescence.

Some Colloid Chemical Aspects and the Overall Development of the Average Particle Number. With regard to developments of the average particle number in the course of the overall polymerization (cf. Figure 3), the interesting question is whether the periods of particle formation and coalescence are clearly separated or both processes taking place concomitantly particularly, during the semibatch period. Or in other words, why does particle formation stop just at the end of the feeding period? Despite the actual reality that an experimental proof of this question is presently not possible, some speculations can be done based on both the experimental data and some more or less reasonable assumptions. Trying to shed light on this question, it is necessary to make assumptions concerning the surfactant self-assembly and adsorption behavior. As the microemulsions prepared utilizing a surfactant mixture and in order to make estimations easier, an "average surfactant molecule" (asm) is defined using the molar ratio of the surfactants in the mixture. The average surfactant molecule is not used for considerations and

Table 2. Characteristic Values of the Average Surfactant Molecule (asm)

	SDS[a]	AOT[b]	asm
M_s (g mol^{-1}) [c]	288.4	444.56	316.2
a_s (nm^2) [d]	∼0.50	∼0.78	∼0.55
cmc (mM)	∼7	∼3	∼6.3

[a] Values justified by the data given in refs 24−27. [b] Values justified by the data given in refs 28 and 29. [c] Molecular weight of the surfactants. [d] Area per surfactant molecule in saturated monolayers.

calculations regarding the formation and composition of the initial microemulsion but is used much more to estimate the number of remaining micelles and the amount of adsorbed surfactant in the course of the reaction where the microemulsion regime is left. The surfactant mixture consists of a mole fraction of SDS and AOT of 53 and 11.5 mM, respectively. The characteristic values of the asm and the values for the pure surfactants in the mixture used for the calculations are put together in Table 2. The average aggregation number in micelles of the asm is assumed to be 80.[26] With these values and the experimentally determined latex characteristics it is possible to estimate changes in the amount of adsorbed asm and in the number of micelles in the course of the polymerizations. This is especially meaningful for the semibatch and the post-addition period as at the end of the batch microemulsion polymerization a huge number of empty micelles is present as it was verified in ref 13. For the above styrene microemulsion polymerizations it was proven that the number of empty micelles at the end of the polymerization is even higher than the initial number of swollen micelles.[19]

Figure 8 shows the calculated changes in the number of micelles (N_m) during the semibatch and post-addition polymerization period for all three initiator concentrations. The number of micelles depends according to relation 6 inversely on the aggregation number of the surfactant and directly on the difference between the micellar surfactant concentration ($\bar{C}_{ms}$) and the amount of the adsorbed surfactant given by $A_p/\bar{a}_s$, where A_p is the overall particle surface and $\bar{a}_s$ is the area covered per asm.

$$N_m \propto \frac{\bar{C}_{ms} - A_p/\bar{a}_s}{\bar{n}_m} \qquad (6)$$

Negative N_m values mean that the polymer particle surface area is larger than the micellar area, and hence the degree of coverage of the polymer particles with surfactant is less than saturation, that is, less than 100%. The curves depicted in Figure 8 have been generated with the parameter set given in Table 2 and a micellar aggregation number $\bar{n}_m = 80$. This parameter set suggests that during the semibatch period the number of micelles vanishes. This is an important piece of information with consequences regarding particle formation as during the whole semibatch period the experimental data show that particles were generated (cf. Figure 3). The crucial parameter in these estimations is $\bar{a}_s$, and hence it was varied in order to see at which values the estimations suggest that N_m stays during the whole duration of the polymerization above zero. For $\bar{a}_s = 1$ nm^2 the calculated number of micelles stays for all initiator concentrations during the whole polymerization time above zero whereas for $\bar{a}_s = 0.8$ nm^2

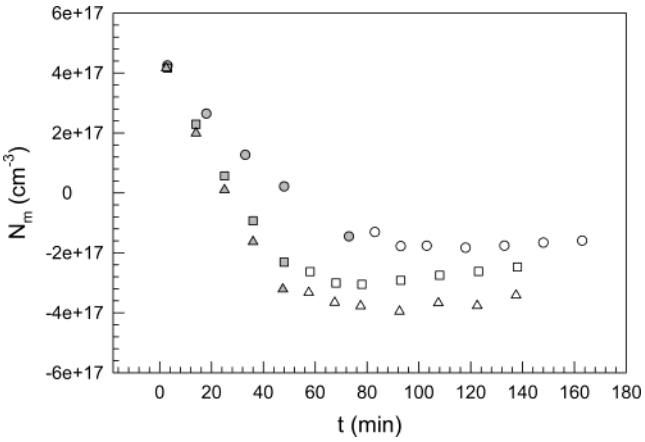

Figure 8. Change of the number of asm micelles (N_m) of during the semibatch and post-addition polymerization period; calculation were performed with the data for the asm given in Table 2 and an average micellar aggregation number of 80. Legends: cf. Figure 1.

N_m drops below zero during the polymerization only for the highest initiator concentration. However, $\bar{a}_s$ values of this order are unreasonably high as for the branched AOT surfactant a value of 0.6 nm^2 has been obtained which is the expected 0.1−0.2 nm^2 higher compared with single chain surfactants with equivalent number of carbon atoms.[24] Consequently, the scenario described by the calculated data depicted in Figure 8 is very likely realistic. This means that during the semibatch microemulsion polymerizations investigated here nucleation of particles occurs regardless whether swollen micelles are present or not. Questions concerning the mechanism of particle nucleation are beyond the scope of this contribution, but some ideas have already been discussed elsewhere,[13] however, without being complete. Unfortunately, it was not possible to get the easy experimental answer whether surfactant micelles are present at the end of the semibatch period by surface tension measurements as described in ref 13. The monomer feed has to come to a halt when the viscosity of the dispersion was so high that an effective mixing with the stirring system became impossible. This high viscosity makes also surface tension measurements to a challenging task, as standard methods cannot be applied to get reliable data. Increasing viscosity of the polymer dispersion during the semibatch polymerization period originates from the increasing particle concentration, which causes rising interactions due to at least two reasons. First, the average distance between the particles (d_{pp}) decreases according to $d_{pp} \propto N_p^{-1/3}$. Second, the ionic strength decreases and hence the Debye screening length (l_D) increases in the course of the polymerization due to covalent binding of peroxodisulfate ions to the polymer particles and due to the adsorption of surface active and counterions to the particle surface and the electric double layer, respectively (cf. above), according to $\lambda_D = 0.01762(T/C_{IS})^{1/2}$, where T is the absolute temperature, C_{IS} is the ionic strength in M, and l_D results in nm. To get an idea about the change in the Debye length, the following considerations might be useful. At the beginning of the polymerization where the total ionic strength is about 10 mM (approximately three-fourths arising from the cmc of the surfactants) l_D is some 3−4 nm. Considering only KPS, l_D is between 12 and 7 nm for the three concentrations. d_{pp} decreases during the semibatch period from above 120 nm to less than 50 and 60 nm

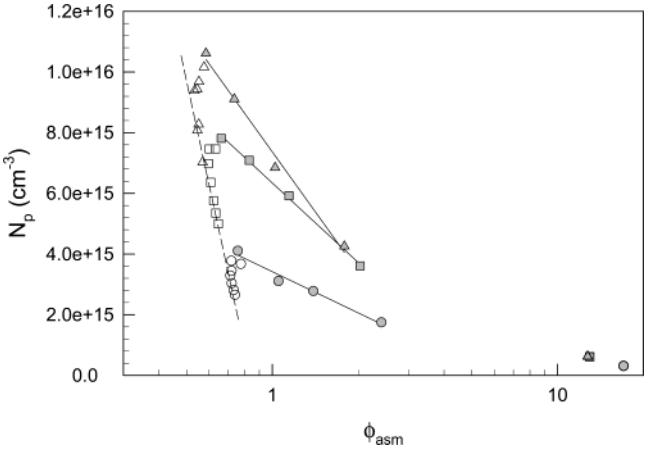

Figure 9. Change in the particle concentration during the semibatch and post-addition polymerization periods in dependence on the ratio between the micellar asm concentration and the amount of asm adsorbed (f_{asm}); the black lines represent linear regressions of the particular periods, and the dashed line is just for guiding the eyes. Legends: cf. Figure 1.

for the highest and lowest initiator concentration, respectively. These data illustrate the changing interactions in the polymer dispersions during the semibatch polymerization periods finding expression in strongly increasing viscosity.

An alternative plot to Figure 8 is the one given in Figure 9 where the experimentally determined number of particles is plotted in dependence on the ratio between the micellar asm concentration and the amount of asm adsorbed (f_{asm}), which is decreasing with progressing polymerization. The semilogarithmic plots reveal some interesting features, which do not change with varying parameters to calculate f_{asm} as the curves will only be shifted along the *x*-axis. The first data points at f_{asm} values above 10 represent the situation at the start of the feeding of additional BA. During the feed period, as long as particles are generated, straight lines are obtained for each KPS concentration. The slope increases with increasing initiator concentration. This experimental fact together with the curves plotted in Figure 8, where the actual number of micelles is higher for the polymerizations with lower initiator concentrations, leads to the conclusion that for the particular conditions the initiator concentration and not the number of micelles determines the particle concentration. Moreover, the curves indicate that there exists obviously a saturation value with regard to the initiator concentration where the generated radical flux is high enough to initiate the maximum number of particles at a given surfactant concentration. For the given surfactant concentration the amount of KPS used in ME3 (0.65 mM) is obviously already very close to that critical concentration.

Other interesting features are to recognize during the last stage of the polymerizations where mainly particle coalescence takes place. After a transient behavior all data points in Figure 9 follow one line. A straightforward explanation for this experimental finding is not available at the moment. Possibly, this behavior can be interpreted that the decrease in the particle area is controlled by the overall surfactant concentration, which is the same for all polymerizations, and thus, the single line represents in some way an adsorption isotherm. Furthermore, it is to be noticed interestingly that the extension of the transition range is larger for higher initiator concentrations. The occurrence of the transition range and the observed dependence on the initiator concentration are consequences of the still ongoing importance of the polymerization reaction in this period of the process whereas at higher conversions the particle coalescence and the influence of the overall surfactant concentration becomes dominating. During the transition range N_p already decreases and the overall particle surface, even if only slightly but still increases.

Coming back to the initial questions of this chapter concerning the overall development of N_p, it can be concluded that the initiator concentration is of dominating influence. During the initial batch and the beginning of the semibatch polymerization period D_p decreases stronger the higher C_I. As estimations suggest that micelles very likely disappear during the semibatch period but particle formation continues during the whole semibatch period, another particle formation mechanism than micellar or droplet nucleation is likely to occur. Immediately after the monomer feed has been stopped particle coalescence takes place as the system tries to reduce its free energy. Interestingly, the rate constant of particle coalescence shows the reverse dependence on the initiator concentration than the slope of the N_p−time curves as long as $dN_p/dt > 0$. The amount of free monomer in the reactor when the BA feed is stopped and also during the whole semibatch period is between 25 and 30% relative to the total amount, and hence, no stable free monomer phase is present but the monomer is distributed between the water phase and the particles and, if present, also micelles. The experimental fact that formation of new particles stops at the same time as the monomer feed is switched of leads on one hand to the conclusion that the monomer concentration in the aqueous phase is crucial for particle formation since the neat BA drops fed into the reactor need a certain period of time to equilibrate among all phases and the equilibration takes place due to diffusion of monomer molecules through the aqueous phase. During the equilibration period the monomer is nonhomogeneously distributed in the continuous phase, as it is higher than the average solubility in water in the vicinity of the BA drops. This conclusion is also in accordance with the above assumption of nonmicellar particle nucleation mechanism. On the other hand, there is no reason that stopping the monomer feed may cause particle coalescence to start. Quite the reverse, stopping the monomer feed should slightly improve particle stabilization, as more stabilizer molecules are available. In summary, these deliberations lead to the logical conclusion that particle nucleation takes place as long as monomer is fed into the reactor that means it stops at the end of the semibatch period. Particle coalescence may take place concomitantly already during the semibatch period and becomes dominating during the post-addition polymerization period.

Average Molecular Weight and Number of Chains per Particle. Because of the compartmentalization effect, microemulsion polymerization is especially suited to form high molecular weight polymers. Figure 10 shows the development of the average molecular weight during the semibatch and the post-addition polymerization period for all three initiator concentrations in dependence on the instantaneous monomer conversion. For all polymerizations two straight lines can describe the development of M_w with conver-

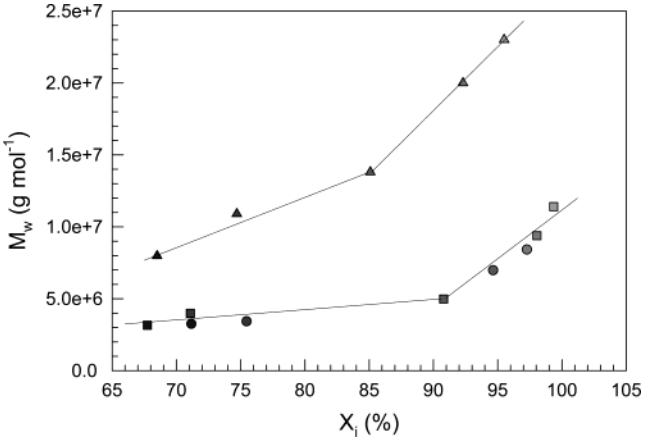

Figure 10. Change of the average molecular weight with instantaneous conversion (X_i) during the semibatch and post-addition polymerization period; the lines are just for guiding the eyes. Legends: circle, ME1 (0.27 mM KPS); squares, ME2 (0.46 mM KPS); triangles, ME3 (0.65 mM KPS).

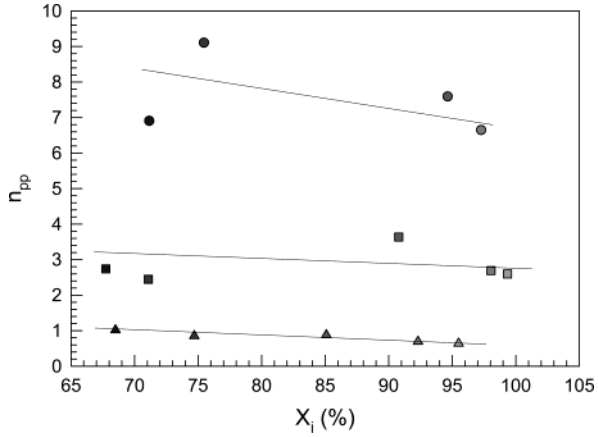

Figure 11. Change of the average number of polymer molecules per particle in dependence on the instantaneous conversion during the semibatch and post-addition polymerization period; the lines are just for guiding the eyes. Legends: cf. Figure 10.

sion whereby the slope is higher in the high conversion range. The data for the two lower initiator concentrations are almost identical at generally lower molecular weights than for the highest C_I. Moreover, the gap between the molecular weights for the highest and the two lower initiator concentrations increases the higher the conversion. This is a typical behavior for polymerizations where chain transfer to polymer plays a crucial role. Its is known that besides chain transfer to monomer in BA free radical polymerization also chain transfer reaction to dead polymer chains takes place.[30−32] Particularly for heterophase polymerization where the polymer concentration in the particles as main reaction locus is very high this reaction is of special importance. The transfer reaction proceeds mainly via abstraction of a hydrogen atom from a tertiary CH bond in BA backbone units. The probability of this kind of chain transfer increases with decreasing monomer concentration (increasing conversion), increasing radical flux (higher initiator concentration), and particularly for heterophase polymerizations with decreasing particle size as it is confirmed by the data depicted in Figure 10. Together with the data from Figure 2, it is possible to calculate the average number of chains per particle (n_{pp}). Despite some scatter with decreasing initiator concentration, the data in Figure 11 confirm the occurrence of chain transfer to polymer as n_{pp} decreases with increasing instantaneous conversion. The chain transfer to polymer obviously overrules the effect of particles coalescence, which should cause an increase in n_{pp}. Other features for n_{pp} are decreasing values with increasing initiator concentration and/or particle size and values of about 1 for the highest initiator concentration. This is much more an effect of chain transfer to polymer than a proof that only one chain is generated per particle in the course of the polymerization. A last remark, confluence of particle during particle coalescence, which is more pronounced at higher than lower conversion, can take place despite the formation of highly branched or even slightly cross-linked particles as the polymerization temperature is for sure above the glass transition temperature.

In conclusion, semibatch microemulsion polymerization of BA with neat monomer feed is useful to improve the emulsifier utilization considerably. For instance, polymer dispersions with polymer mass fraction of almost 30 wt % and particle sizes below 40 nm at surfactant amounts between 5 and 6 wt % are easily accessible. This is a considerable improvement compared with batch microemulsion polymerization and the above parameters absolutely comparable with that for normal emulsion polymerizations leading to particles with similar sizes as those obtained in this investigation. Moreover, the particular polymerization investigated shows interesting features regarding both heterophase polymerization kinetics and colloid chemical properties such as particle nucleation at high instantaneous conversion in dependence on whether monomer feed takes place and particle growth during the post-addition period dominated by particle coalescence processes.

Acknowledgment. A.G.R. acknowledges a fellowship from the DAAD (Bonn, Germany) and CONACYT (México). We are grateful to Dr. G. Rother for any kind of help during the determination of the molecular weight by static light scattering. Moreover, the authors thank the Max Planck Society and the Max Planck Institutes of Colloids and Interfaces for the opportunity use of all the facilities and analytical equipment needed.

References and Notes

(1) Xu, X.; Fei, B.; Zhang, Z.; Zhang, M. *J. Polym. Sci., Part A: Polym. Chem.* **1996**, *34*, 1657−1661.
(2) Xu, X.; Zhang, Z.; Wu, H.; Ge, X.; Zhang, M. *Polymer* **1998**, *39*, 5245−5248.
(3) Gan, L. M.; Lian, N.; Chew, C. H.; Li, G. Z. *Langmuir* **1994**, *10*, 2197−2201.
(4) Taylor, M. A. In *Polymer Dispersions and Their Industrial Applications;* Urban, D., Takamura, K., Eds.; Wiley-VCH: Weinheim, 2002; pp 15−40.
(5) Blam, A. F.; Yang, Y. C.; Shah, P. K. EP 391 343, published 10.10.1990 to B.F. Goodrich Co.
(6) Roy, S.; Devi, S. *Polymer* **1997**, *38*, 3325−3331.
(7) Rabelero, M.; Zacarias, M.; Mendizabal, E.; Puig, J. E.; Dominguez, J. M.; Katime, I. *Polym. Bull. (Berlin)* **1997**, *38*, 695−700.
(8) Ming, W.; Jones, F. N.; Fu, S. *Macromol. Chem. Phys.* **1998**, *199*, 1075−1079.
(9) Ming, W.; Jones, F. N.; Fu, S. *Polym. Bull. (Berlin)* **1998**, *40*, 749−756.
(10) Xu, X. J.; Chew, C. H.; Siow, K. S.; Wong, M. K.; Gan, L. M. *Langmuir* **1999**, *15*, 8067−8071.
(11) Sosa, N.; Peralta, R. D.; Lopez, R. G.; Ramos, L. F.; Katime, I.; Cesteros, C.; Mendizabal, E.; Puig, J. E. *Polymer* **2001**, *42*, 6923−6928.
(12) Braun, O.; Selb, J.; Candau, F. *Polymer* **2001**, *42*, 8499−8510.
(13) Tauer, K.; Ramírez, A. G.; López, R. G. *C. R. Chim.*, in press.

(14) Tauer, K.; Reinisch, G.; Gajewski, H.; Müller, I. *J. Macromol. Sci., Chem.* **1991**, *A28*, 431−460.
(15) Evans, D. F.; Wennerström, H. *The Colloidal Domain*; VCH: Weinheim, 1994; pp 110−127, 333−338.
(16) Matijevic, E.; Pethica, B. A. *Trans. Faraday Soc.* **1958**, *54*, 1382−1389.
(17) Tajima, K. *Bull. Chem. Soc. Jpn.* **1971**, *44*, 1767−1771.
(18) Kralchevsky, P. A.; Danov, K. D.; Broze, G.; Mehreteab, A. *Langmuir* **1999**, *15*, 2351−2365.
(19) Full, A. P.; Kaler, E. W.; Arellano, J.; Puig, J. E. *Macromolecules* **1996**, *29*, 2764−2775.
(20) Tauer, K. Kühn, I. *Macromolecules* **1995**, *28*, 2236−2239.
(21) Tauer, K.; Kühn, I. In *Polymeric Dispersions: Principles and Applications;* Asua, J. M., Ed.; Kluwer Academic Publishers: Dordrecht, 1997; pp 49−65.
(22) Maeder, S.; Gilbert, R. G. *Macromolecules* **1998**, *31*, 4410−4418.
(23) Friis, N.; Hamielec, A. E. *J. Appl. Polym. Sci.* **1975**, *19*, 97−113.
(24) Mysels, K. J.; Princen, L. H. *J. Phys. Chem.* **1959**, *63*, 1696−1700.
(25) Rehfeld, S. J. *J. Phys. Chem.* **1967**, *71*, 738−745.
(26) Hayter, J. B.; Penfold, J. *Colloid Polym. Sci.* **1983**, *261*, 1022−1030.
(27) Turner, S. F.; Clark, S. M.; Rennie, A. R.; Thirtle, P. N.; Cooke, D. J.; Li, Z. X.; Thomas, R. K. *Langmuir* **1999**, *15*, 1017−1023.
(28) Li, Z. X.; Lu, R.; Thomas, R. K.; Penfold, J. *J. Phys. Chem. B* **1997**, *101*, 1615−1620.
(29) Nave, S.; Eastoe, J.; Penfold, J. *Langmuir* **2000**, *16*, 8733−8740.
(30) Lovell, P. A.; Shah, T. H.; Heatley, F. *Polym. Commun.* **1991**, *32*, 98−103.
(31) Lovell, P. A.; Shah, T. H.; Heatley, F. *ACS Symp. Ser.* **1992**, *492*, 188−202.
(32) Lovell, P. A. In *Emulsion Polymerization and Emulsion Polymers;* Lovell, P. A., El-Aasser, M. S., Eds.; Wiley: Chichester, 1997; pp 239−276.

MA030218G